Sustainable Cities and Society xxx (xxxx) xxx

Contents lists available at ScienceDirect

Sustainable Cities and Society

journal homepage: www.elsevier.com/locate/scs

Moving beyond exposure: a globally comparable framework for heat risk assessment in cities

Nethmi Jayaratne Kariyawasam [a,b,*], Jesus Lizana [a,c], Radhika Khosla [a,b]

[a] ZERO Institute, University of Oxford, Oxford OX2 0ES, United Kingdom
[b] Smith School of Enterprise and the Environment, School of Geography and the Environment, University of Oxford, Oxford OX1 3QY, UK
[c] Department of Engineering Science, University of Oxford, Parks Road, Oxford OX1 3PJ, UK

ARTICLE INFO

Keywords:
Heat risk
Cooling degree days
Climate adaptation
Extreme heat
Cooling

ABSTRACT

Most global heat assessments rely on exposure-only indicators. However, heat risk in cities extends beyond climatic extremes and is mediated by social vulnerabilities and infrastructural capacities that determine how populations experience and respond to heat. Here, we map heat risk globally in cities with populations over one million using a harmonised composite index disaggregated into hazard exposure, vulnerability, and coping capacity. Hazard exposure is characterised using the population-weighted Universal Thermal Climate Index (UTCI)-based Cooling Degree Days, which capture cumulative heat stress. Vulnerability and coping capacity are characterised by economic capacity, demographic structure, and infrastructural factors. The results show that over 95% of the highest-risk cities are concentrated in South and Southeast Asia and Sub-Saharan Africa. They also demonstrate that exposure alone is insufficient to predict risk. Several highly exposed cities (e.g., Bangkok, Jeddah) rank lower due to strong coping capacity, while others (e.g., Karachi, Faisalabad, Kaduna) face severe risk under moderate exposure. Our component-resolved risk analysis also reveals within-region heterogeneity, highlighting the need for spatially resolved, socio-economically contextualised approaches to heat adaptation by reducing exposure, addressing socioeconomic vulnerability, and investing in infrastructure to advance urban heat resilience in a rapidly warming world.

1. Introduction

Extreme heat is emerging as one of the most dangerous and inequitable consequences of climate change (International Panel on Climate Change (IPCC), 2023). Heatwaves are increasing in frequency, duration, and intensity, driving excess mortality, infrastructure failures, and economic losses in cities worldwide (Ebi et al., 2021; Mora, Dousset, et al., 2017; World Bank, 2025). With over half of the global population currently residing in cities and projections indicating that two-thirds will do so by 2050, cities are becoming critical hotspots of climate impact (United Nations Department of Economic and Social Affairs, 2019). Cities face compound risk due to anthropogenic warming, land cover modification, population density and socio-economic disparities, which amplify the effects of rising temperatures (Jones, 2025; Tuholske et al., 2021). The 2022 IPCC report highlights that urban populations are at "disproportionately high risk" from rising temperatures, especially in areas where adaptive capacity is limited (IPCC, 2023).

Despite this growing threat, most global assessments of heat risk in cities remain exposure-centric, relying on land surface temperature, heatwave metrics, heatwave frequency, or urban heat island intensity as proxies (D. Li & Bou-Zeid, 2013; L. Zhao et al., 2018). However, these measures capture only a partial view of the problem, as they describe climatological extremes without accounting for the social and infrastructural factors that shape impacts (Ye & Yang, 2025). This limitation is at odds with the IPCC's conceptualisation of risk, which emphasises that risk emerges from the interaction between hazard exposure, vulnerability, and response capacity (IPCC, 2023).

In response to the limitations of exposure-only approaches, recent studies have adopted composite heat vulnerability and risk indices that integrate social, demographic, economic, and built-environment dimensions across urban scales (Kumari R & Kitchley, 2024; Xiang et al., 2022; Xu et al., 2025). These include Heat Vulnerability Indices (HVI), which combine demographic sensitivity, socio-economic disadvantage,

* Corresponding author at: School of Geography and the Environment, S Parks Rd, Oxford, OX1 3QY, United Kingdom.
E-mail addresses: nethmi.jkariyawasam@ouce.ox.ac.uk (N. Jayaratne Kariyawasam), jesus.lizana@eng.ox.ac.uk (J. Lizana), radhika.khosla@smithschool.ox.ac.uk (R. Khosla).

https://doi.org/10.1016/j.scs.2026.107535
Received 1 February 2026; Received in revised form 20 May 2026; Accepted 20 May 2026
Available online 21 May 2026
2210-6707/© 2026 The Author(s). Published by Elsevier Ltd. This is an open access article under the CC BY license (http://creativecommons.org/licenses/by/4.0/).

and environmental exposure; and Social Vulnerability Index (SoVI)-type approaches, which emphasise structural inequalities such as poverty, age, and access to services (Bao et al., 2015; Mah et al., 2023). More recent work extends this perspective by introducing concepts such as Summer Energy Poverty and Systemic Cooling Poverty, highlighting how access to and affordability of infrastructure, among other variables, shape households' capacity to cope with extreme heat (Z. Chen et al., 2025; Mazzone et al., 2023). While these approaches have significantly advanced understanding of urban heat vulnerability and socio-economic inequality, most applications remain focused on individual cities or regional contexts, with limited comparability across regions and nations. Studies such as Kumari R & Kitchley (2024), Uejio et al. (2011), Xiang et al. (2022) and Xu et al. (2025) provide detailed place-based assessments using locally tailored socio-demographic, environmental, and built-environment indicators that are closely aligned with local urban conditions. Some studies have extended HVI-type approaches across multiple cities, including comparative assessments across Indian cities (Rathi et al., 2022) and Australian capital cities (F. Li et al., 2024). However, even these comparative applications rely on region-specific datasets and locally adapted indicator weighting schemes, limiting methodological consistency and direct comparability across diverse urban settings globally. Consequently, despite important advances in composite heat-vulnerability assessment, existing HVI- and SoVI-type approaches remain limited in their capacity to support globally harmonised and directly comparable city-scale heat-risk assessment. To address this gap, the present study builds on the INFORM risk framework to develop a globally harmonised, heat-specific, component-resolved assessment using consistent datasets and methods across cities.

More broadly, cities with similar thermal profiles may experience vastly different health and infrastructure outcomes, depending on the social and physical systems in place (Rocha et al., 2024). Environmental factors further complicate this picture: vegetation loss, for example, can intensify moist-heat stress in cities, reinforcing the need to include ecological buffers as determinants of risk (Du et al., 2025; Y. Li et al., 2024). Taken together, these insights point to a more integrated understanding of risk as emerging from the intersection of hazard exposure, socio-demographic and economic vulnerability, and the capacity of systems to cope or adapt (IPCC, 2023; Vernaccini & Poljansek, 2017), a dynamic often overlooked in hazard-exposure-only approaches.

Cities with moderate heat exposure may nonetheless suffer disproportionate impacts due to high levels of poverty, ageing populations, limited green cover, or unaffordable cooling infrastructure (Du et al., 2025; Hondula et al., 2015; UCCRN, 2018). Vulnerable groups, including older adults, children, informal workers and people with pre-existing conditions, are consistently shown to face elevated risks of heat-related illness and mortality, regardless of absolute temperatures (Mitchell et al., 2016; Watts et al., 2017). Moreover, the spatial distribution of vulnerability within cities means that some neighbourhoods may experience far worse outcomes during heat events than others, even when ambient temperatures are comparable. This heterogeneity highlights the need for composite risk frameworks with spatially resolved socially contextualised risk assessments (IPCC, 2023; Vernaccini & Poljansek, 2017).

Despite these advances, very few studies have operationalised this composite perspective to account for socio-demographic vulnerability, adaptive capacity and hazard metrics at the global city scale, despite calls for scalable frameworks and typologies to generalise insights across diverse urban contexts (Creutzig et al., 2025). The tendency to prioritise physical metrics in global modelling efforts may lead to underestimating or misidentifying the areas of highest need. Several recent global efforts have mapped urban heat exposure or climate hazard risk, including high-resolution population–heat exposure datasets (Tuholske et al., 2021) and global projections of deadly heat events (Mora, Dousset, et al., 2017). While these studies have highlighted regions such as South Asia and West Africa as heat hotspots, they rely primarily on hazard or exposure indicators and cannot fully capture the moderating effects of vulnerability and coping capacity (Klein & Anderegg, 2021). Other indices, such as the Notre Dame Adaptation Initiative (ND-GAIN, 2021) urban adaptation index or national-scale INFORM (Vernaccini & Poljansek, 2017) risk scores provide insight into socio-economic fragility and systemic risk, but are typically available at the national scale and for multi-hazard contexts, rather than consistent comparison across cities globally.

Taken together, existing approaches remain limited by three key challenges: (i) limited global comparability across cities due to differences in data sources, spatial scales, weighing schemes and indicator selection; (ii) limited integration of hazard exposure, vulnerability, and coping capacity within a globally consistent, heat-specific framework; and (iii) limited ability to compare how different combinations of these risk components shape city-level heat-risk pathways and inform policy-relevant assess. Addressing these gaps requires a harmonised framework that enables direct cross-city comparison while disentangling the relative contributions of different risk dimensions. Our work bridges these gaps by combining high-resolution city-level data with the INFORM framework to deliver a globally harmonised multidimensional, heat-specific risk assessment at the city scale that extends composite vulnerability indices beyond local and regional applications by explicitly distinguishing hazard exposure, vulnerability, and lack of coping capacity, thereby enabling component-level attribution of distinct city-level heat-risk drivers.

The urgency of integrating vulnerability and capacity into risk models to inform targeted interventions is increasingly evident. During the late-June to early-July 2025 heatwave, an estimated 2,305 excess deaths occurred across 12 major European cities with a combined population of over 30 million people, and more than 80% of these deaths were among adults aged 65 years and older (Clarke et al., 2025). Looking ahead, projections indicate that heat-related mortality in Europe will rise sharply, driven not only by intensifying climate hazards but also by demographic shifts, particularly population ageing (Wu et al., 2025).

In this study, we adopt the INFORM Risk Index (Vernaccini & Poljansek, 2017), a composite framework developed by the European Commission, to assess heat risk at the city-scale, integrating heat-specific hazard indicators with socio-demographic vulnerability and coping capacity, enabling globally consistent, component-resolved risk diagnostics. Our approach builds on the recent methodological advances, including the European Commission's Risk and Vulnerability Assessment Guide (Palermo et al., 2025), which also employs a multi-dimensional framework encompassing hazard, vulnerability and adaptive capacity.

In line with recent methodological guidance (IPCC, 2023; Palermo et al., 2025), hazard exposure refers to the intensity and spatial extent of heat related conditions affecting urban populations; vulnerability refers to the propensity of exposed populations to experience harm, shaped by socio-demographic and economic characteristics such as age, health status, and socio-economic disadvantage; and coping capacity as the ability of a system to manage and absorb adverse impacts in the short term, and to build adaptive capacity, which reflects a system's longer-term ability to adjust, learn, and transform in response to evolving climate risks. While both are critical to resilience, coping capacity refers to immediate, tangible assets such as cooling infrastructure and urban greenery, whereas adaptive capacity encompasses broader factors such as institutional readiness, technological access, and social equity.

This framework is aligned with the recently growing body of literature, which identifies a broad range of determinants shaping heat vulnerability and coping capacity, including informal housing prevalence, building materials, occupational exposure, urban density, access to healthcare, and the spatial distribution of green and cooling infrastructure (Kumari R & Kitchley, 2024; Xiang et al., 2022; Xu et al., 2025). While these dimensions are conceptually important, their

availability and comparability remain uneven at the global city scale.

The integrated framework we present enables globally consistent, spatially explicit, and socially contextualised comparisons of city-level heat risk, allowing cross-city comparison of the relative roles of hazard exposure, vulnerability, and coping capacity, providing a diagnostic basis to inform urban adaptation planning. Building on this framework, the paper makes two primary contributions:

- First, it develops a globally consistent, city-scale heat risk framework that integrates cumulative heat stress, socio-demographic vulnerability, and coping capacity within a single, component-resolved framework across large cities globally. In contrast to many existing HVI- and SoVI-type approaches, which are often locally calibrated, this enables systematic cross-city comparison while revealing how different combinations of hazard exposure, vulnerability, and infrastructural capacity shape risk outcomes.
- Second, by disaggregating composite risk into its underlying components, the analysis enables empirical comparison of distinct pathways to high heat risk across cities, demonstrating where risk is driven primarily by exposure, amplified by social vulnerability, or by limited coping capacity. This component-level insight provides a practical basis for targeting adaptation strategies to local risk drivers rather than applying uniform, hazard-focused responses.

The article is structured as follows. Section 2 describes the data sources and methodological approach used. Section 3 presents the global results, including the spatial distribution of heat risk across cities and a component-resolved analysis highlighting regional patterns and intra-regional heterogeneity. Section 4 discusses the implications of these findings for urban heat adaptation, contextualises the results within the broader literature and policy landscape, and highlights the study limitations. Finally, Section 5 concludes by summarising the key insights, outlining policy relevance, and directions for future research.

2. Materials and methods

The adapted heat risk framework in the study is summarised in Fig. 1, which provides an overview of the three core dimensions of risk (hazard exposure, vulnerability, and lack of coping capacity) and their constituent indicators used in the city-level assessment. Together, these dimensions reflect the systemic nature of urban heat risk, in which climatic stress interacts with social sensitivity and infrastructural capacity to shape observed impacts across cities. A summary of the selected indicators is presented below.

Hazard exposure is represented by population-weighted cooling degree days (CDD) derived from UTCI, together with land surface temperature (LST) anomalies that capture spatial patterns of thermal intensity. The UTCI is a heat stress metric that integrates air temperature, humidity, wind, and mean radiant temperature to provide a physiologically relevant measure of heat stress. It has been widely applied in both global and city-scale assessments of heat risk and health impacts (Di Napoli et al., 2018; Jian et al., 2024). UTCI-based CDDs measure cumulative outdoor heat stress by comparing daily UTCI values with a reference threshold (usually 65 °F or 18 °C) (Chakraborty et al., 2019; N. Zhao et al., 2017).

Vulnerability is characterised by demographic age structure (proportion of children < 4 and adults > 65) and economic capacity (inverse GDP per capita), reflecting consistent evidence that children and older adults experience elevated heat-related morbidity and mortality due to physiological susceptibility (Gasparrini et al., 2015; Masselot et al., 2023) and that lower-income groups face disproportionate exposure and limited adaptation options (Uejio et al., 2011; Voelkel et al., 2018). Air-conditioning (AC) penetration is also treated as part of vulnerability, as it is a key determinant of reduced heat-related mortality at the individual or household level, while unequal access to it reflects socio-economic susceptibility to heat impacts (L. Davis et al., 2021; L. W. Davis & Gertler, 2015; Mora, Counsell, et al., 2017);

Finally, the lack of coping capacity is captured by the fraction of vegetation cover (expressed as Normalised Difference Vegetation Index (NDVI) and Fractional Tree Cover (FTC)), and electricity costs. Vegetation cover mitigates outdoor heat via shade and evapotranspiration and is strongly associated with lower exposure and mortality (Du et al., 2025; Y. Li et al., 2024). Electricity costs act as potential barriers or enablers to cooling access for low and high-electricity-intensive cooling technologies (e.g., fans, evaporative coolers and ACs), constraining households' ability to mitigate thermal stress (Falchetta et al., 2024; Mazzone et al., 2023).

The selected indicators are both theoretically grounded and consistently available across globally harmonised, city-comparable datasets, enabling systematic cross-city analysis of near-term resilience. We further acknowledge that coping capacity is inherently multidimensional and that not all relevant dimensions are consistently represented at this scale yet. More details about the indicator selection process for this study are provided in the Supplementary Note 2, including indicators excluded due to data constraints and those reserved for future work.

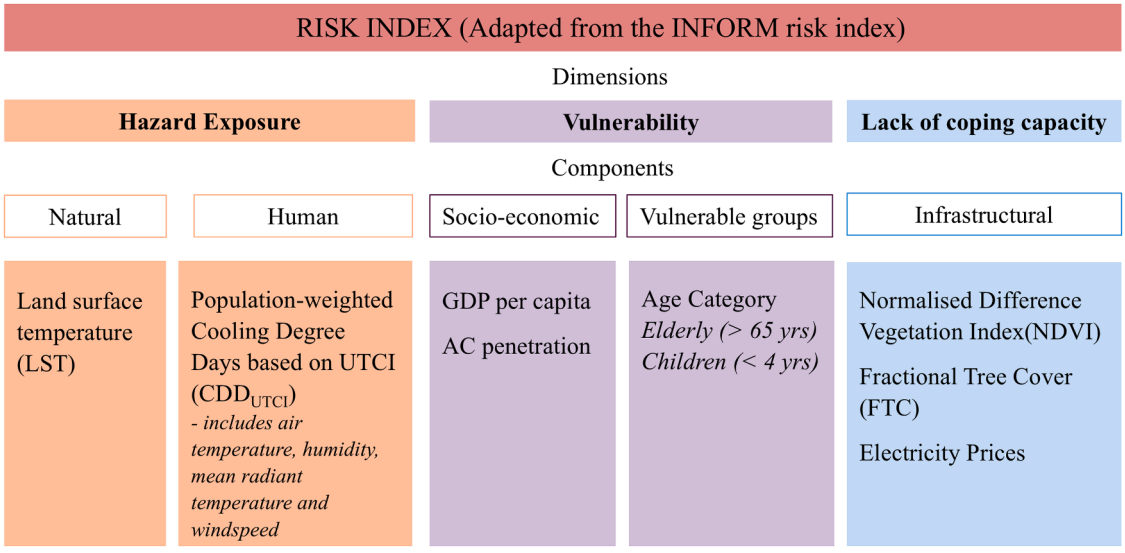

Fig. 1. Risk dimensions and components of the adapted framework.

The materials and methods used to operationalise this framework and derive the city-level heat risk index are further described below.

2.1. Material

All data inputs were sourced from publicly available, peer-reviewed, or institutional datasets with global coverage. All datasets used are listed in Table 1, categorised by hazard exposure, vulnerability, lack of coping capacity, and boundaries.

2.2. Methods

2.2.1. City heat risk framework

This study presents a global comparative assessment of heat risk for cities with populations exceeding one million, encompassing 205 cities worldwide. Heat risk in cities is conceptualised as a composite function of three interrelated dimensions: hazard exposure, vulnerability, and lack of coping capacity, consistent with the INFORM Risk Index framework, the Sendai Framework for Disaster Risk Reduction, and the IPCC's systemic risk approach (IPCC, 2023; Vaño et al., 2025; Varquez et al., 2025; Vernaccini & Poljansek, 2017).

To reflect the multiplicative interactions inherent in systemic risk processes, the composite heat risk score is calculated as the geometric mean of the three dimensions, following the INFORM Risk Index methodology described in Eq. (1):

$$\text{Risk} = H^{1/3} \times V^{1/3} \times C^{1/3} \quad (1)$$

where H is the hazard exposure score, V is the vulnerability score, and C is the lack of coping capacity score. This geometric mean approach ensures a balanced view of risk by requiring that (1) hazard exposure, (2) vulnerability, and (3) lack of coping capacity are all taken into account, rather than focusing on just one dimension. It highlights that the hazard itself does not solely determine risk, but also the extent to which the system is exposed to it and how prepared or unprepared the system is to respond. Because the factors are multiplied together, a very high value in any one of them can significantly amplify the overall risk, underscoring the importance of addressing each component. The robustness of this aggregation choice is further assessed by comparing it with an additive formulation, which shows high consistency in city rankings. See Supplementary Note 3.

2.2.2. Spatio-temporal resolution

The analysis was conducted using a harmonised spatial framework covering 205 global cities, each with a population of at least 1 million. City boundaries were delineated based on population-weighted urban extents, allowing composite risk estimates to reflect the spatial distribution of urban populations, while recognising that some intra-urban variability may not be fully captured. The urban areas are delineated using the LandScan Urban Areas dataset from Natural Earth (version 4.0.0) (Patterson & Kelso, 2012). This dataset uses the Oak Ridge National Laboratory's LandScan population grid to delimit urban areas globally at approximately 1 km^2 resolution. In this dataset, urban areas are defined as contiguous grid cells exceeding a population density threshold of 200 persons/km^2, while cells with fewer than 200 persons/km^2 are discarded (classified as rural). The spatial extent of each urban area was used to calculate the city statistics for the study. In this context, "cities" refers to urban areas that may include multiple adjacent municipalities.

For each city, risk components are derived from gridded indicators at their native spatial resolutions (≈1–11 km), aggregated over the urban extent using indicator-appropriate. Thus, each city-level score summarises the distribution of high-resolution values across all grid cells within the urban area, enabling globally consistent cross-city comparison, and reflects the finest globally consistent datasets currently available for these dimensions. This approach enables a robust, globally comparable assessment of heat risk across cities. It should be noted that neighbourhood-scale inequalities are not captured in the present analysis.

2.2.3. Indicator selection and normalisation

Each risk dimension comprises a curated set of indicators selected based on their relevance to urban heat risk, global data availability, and methodological alignment with established disaster risk frameworks (IPCC, 2023; Vernaccini & Poljansek, 2017). The resulting indicators define a core set for consistent cross-city comparison, rather than an exhaustive account of all absolute values of determinants influencing urban heat risk. As such, this framework represents a starting point for operationalising multidimensional urban heat risk in a globally comparable way.

Building on this, to ensure cross-dimensional and cross-city comparability, all indicators were normalised to a common 0–1 scale based on their empirical ranges across the full urban sample. The direction of normalisation was determined by the indicator's relationship to each dimension of hazard exposure, vulnerability and lack of coping capacity as described in Eq. (2) and Eq. (3):

$$\text{For positively associated indicators}: \ \text{X\_norm} = \frac{(X - Xmin)}{(Xmax - Xmin)} \quad (2)$$

$$\text{For inversely associated indicators}: \ \text{X\_norm} = \frac{(Xmax - X)}{(Xmax - Xmin)} \quad (3)$$

2.2.4. Calculation of risk components

Within each dimension of hazard exposure, vulnerability and lack of coping capacity, the normalised variables (0–1) were aggregated using

Table 1
Summary of data sources used for the analysis. References refer to the raw datasets used to derive the variables selected, which may involve additional processing or calculations.

	Variable	Spatial resolution	Temporal domain	File format	Reference
Hazard Exposure	Population-weighted Cooling Degree Days from Universal Thermal Climate Index (CDD_{UTCI})	11 km	2020	GeoTIFF	UTCI data: Jian et al. (2024)
		1 km	2020	GeoTIFF	Population data: WorldPop (2018)
	Land surface temperature (LST)	5.5 km	2020	GeoTIFF	Wan et al. (2021)
Vulnerability	GDP per capita	10 km	2020	GeoTIFF	Kummu et al. (2025)
	AC penetration	1 km	2020	GeoTIFF	Falchetta et al. (2024)
	Age category	1 km	2020	GeoTIFF	WorldPop (2018)
Lack of coping capacity	Normalized Difference Vegetation Index (NDVI)	1 km	2020		Didan (2015)
	Fractional Tree Cover (FTC)		2020	GeoTIFF	Liu et al. (2024)
	Electricity prices	National Average	2019	GeoTIFF	World Bank Group (2021)
Boundaries	Urban boundaries	-	-	Shapefile	Florczyk A.J. et al. (2019)
Population	Population data	1 km	2020	GeoTIFF	WorldPop (2018)

arithmetic means, followed by geometric aggregation of the three dimensions to derive the final composite index. Equal weighting was applied across all indicators and dimensions (Vernaccini & Poljansek, 2017). Table 2 summarises the units used to assess each city's performance on the targeted risk component and presents the minimum, median, and maximum results for each city.

Hazard Exposure (H):

This dimension captures both the thermal intensity of urban environments and the degree of population exposure. The hazard exposure score (**H**) was computed as the arithmetic mean of two remote sensing-based indicators: the normalised annual number of population-weighted Cooling Degree Days (CDD_{UTCI}), calculated using the UTCI including all environmental variables affecting thermal stress (dry-bulb temperature, relative humidity, air speed, and mean radiant temperature) and the normalised annual mean land surface temperature(LST) as shown in Eq. (4).

$$\mathbf{H} = \mathbf{Mean}(\text{Population} - \text{weighted}\, CDD_{UTCI}, LST) \quad (4)$$

CDD_{UTCI} was calculated using a mean degree-hour approach (CIBSE, 2006), summing hourly UTCI exceedances above a reference threshold ($\theta_{b=}$ 18°C) across all hours in a day and dividing by 24 to yield daily degree-days as shown in Eq. (5):

$$D_i = \frac{\sum_{j=1}^{24}\left[\theta_{0,j} - \theta_b\right]}{24},\ \theta_{0,j} > \theta_b \quad (5)$$

where:

D_i is the daily cooling degree-days, θ_b is the reference threshold (18°C), and $\theta_{0,j}$ is the hourly UTCI in hour *j*. When $\theta_{0,j} < \theta_b$ the term is set to zero. Annual CDD was then obtained by summing D_i across all days of the year.

In this study, the 18°C threshold is used as a standard comparative reference within a degree-day framework rather than as a universal epidemiological threshold for heat-health risk. As thermal thresholds vary across climatic and socio-cultural contexts, we tested sensitivity by recalculating CDD_{UTCI} using 20°C and 22°C; results are reported in Supplementary Note 4. The analysis shows that, because this is a global comparison with CDD-based normalised data, the choice of threshold has limited influence on the results. As long as the underlying distribution used for normalisation remains consistent, varying the threshold does not substantially alter the overall patterns or conclusions.

Table 2
Summary of the variables.

	Variable	Unit per city	Minimum	Median	Maximum
Hazard Exposure	CDD_{UTCI}	Population-weighted mean (degree days)	86	1467	4764
	LST	Area-weighted mean (K)	279	301	314
Vulnerability	GDP per capita	Area-weighted mean USD (PPP)	808	8335	84502
	Adults>65 years	Percentage (%)	0.01	0.09	0.3
	Children<4 years	Percentage (%)	0.03	0.07	0.17
	AC penetration	Area-weighted mean	0.04	0.41	0.92
Lack of coping capacity	NDVI	Area-weighted mean	0.09	0.38	0.56
	Fractional Tree Cover (FTC)	Percentage (%)	0	1.54	32.06
	Electricity prices	Area-weighted mean USD (PPP)	0.06	0.26	0.86

Vulnerability (V):

Vulnerability captures demographic and socioeconomic conditions that increase susceptibility to heat-related illness and mortality. It is based on the arithmetic mean of three indicators: Inverse GDP per capita (INGDPpc) reflecting the economic capacity, proportion of population under the age of 4 (Children<4) and the proportion of population over the age of 65 (Adults>65), and inverse air conditioning penetration (INAC pene) as shown in Eq. (6).

$$\mathbf{V} = \mathbf{Mean}(\text{INGDPpc}, \text{Children} < 4, \text{Adults} > 65, \text{INACpene}) \quad (6)$$

Lack of Coping Capacity (C):

This dimension reflects limited infrastructure, ecological buffers, and financial means to mitigate or adapt to urban heat. It includes the arithmetic mean of three indicators: inverse Normalised Difference Vegetation Index (INNDVI), inverse fractional tree cover (INFTC), and electricity price adjusted for PPP (Elec_price) as described in Eq. (7).

$$\mathbf{C} = \mathbf{Mean}(\text{INNDVI}, \text{INFTC}, \text{Elec\_price}) \quad (7)$$

2.2.5. Sensitivity analysis

To evaluate the robustness of the index to key methodological assumptions, we conducted sensitivity analyses using alternative weighting schemes, an additive aggregation alternative (Supplementary Note 3), and alternative thresholds for CDD (18°C, 20°C and 22°C, Supplementary Note 4). Robustness was assessed using changes in city rankings, Spearman rank correlations, top-decile overlap, and comparison of risk-score distributions.

3. Results

3.1. The highest heat risk is concentrated in South Asia and Sub-Saharan Africa

The global assessment of cities with more than 1 million inhabitants reveals the range of cities at risk of heat, as shown in Fig. 2.

The results show that over 95% of cities above the 90th percentile in composite heat risk, facing the combined burden of hazard exposure, socio-demographic vulnerability, and limited coping capacity, are located in South and Southeast Asia and Sub-Saharan Africa, highlighting the disproportionate clustering of heat risk in these regions. Specifically, India, Pakistan, Nigeria and Ghana host the largest number of cities with the composite risk scores exceeding the 90th percentile. The ranking for the top 50 cities is provided in Appendix A, with the full ranking in Supplementary Note 1.

These spatial patterns are consistent with those reported in the World Bank Handbook on Urban Heat Management in the Global South (World Bank, 2025), which highlights these regions as priority areas for heat resilience planning. Our analysis advances this evidence base by systematically quantifying a globally consistent, city-level heat-risk index and disaggregating it into its three components. This approach is consistent with broad regional trends and also reveals substantial intra-regional heterogeneity, distinguishing cities where risk is driven primarily by exposure from those where vulnerability or weak coping capacity dominate. The convergence of demographic pressure, limited urban infrastructure, and high thermal exposure renders many of these cities as fragile to heat, motivating a closer examination of the underlying risk components.

3.2. High exposure does not always translate to high risk

While hazard exposure is a critical component of risk, it is not

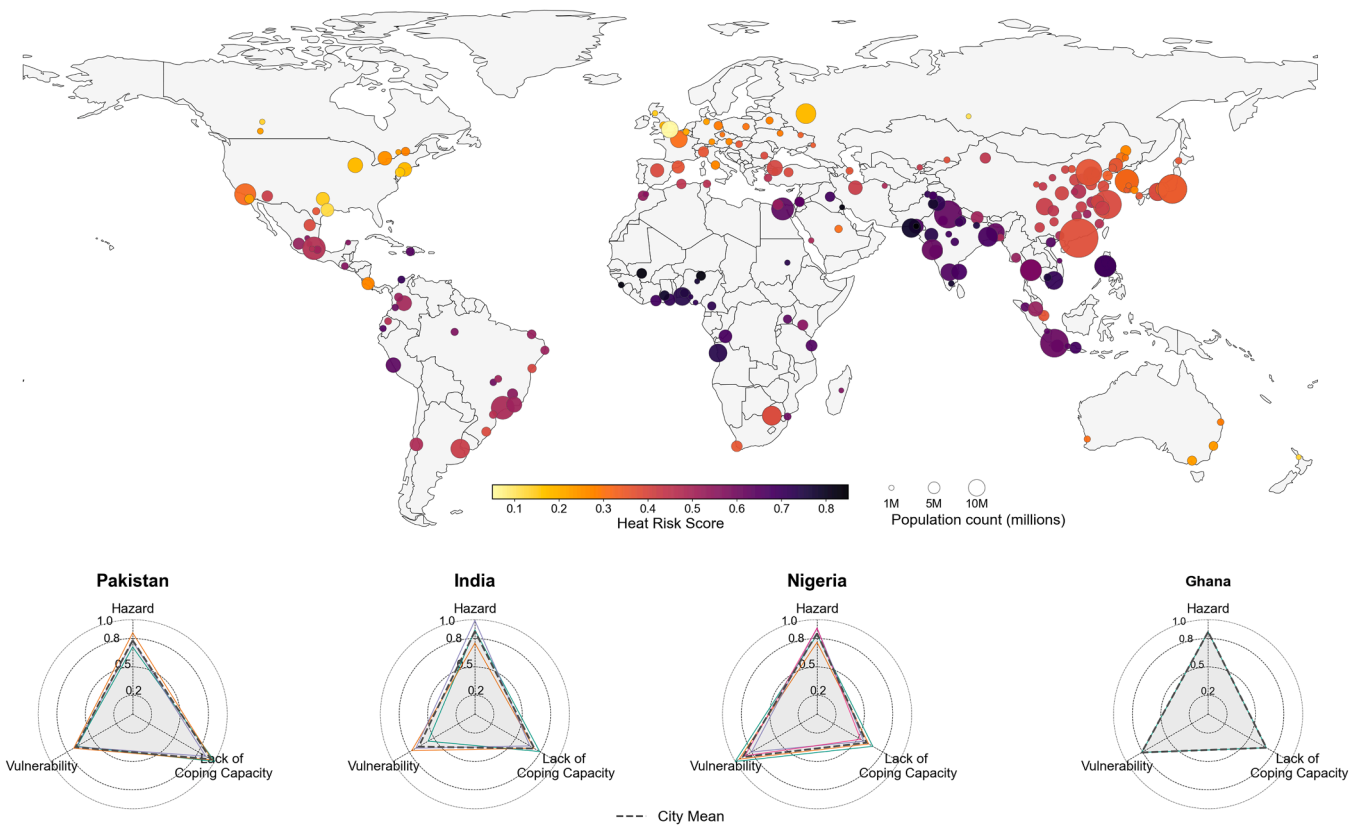

Fig. 2. Global mapping of composite heat risk across cities worldwide with populations exceeding 1 million in 2020. a, Global map displaying composite heat risk scores for cities, where bubble size represents population. b, Radar plots show national-level means for hazard exposure, vulnerability, and lack of coping capacity for the cities at the highest risk, exceeding the 90th percentile of the risk score, in Pakistan, India, Nigeria, and Ghana. The dashed lines represent the mean values across the high-risk cities within each country. The radial axes indicate the relative intensity of each dimension, enabling comparison of risk profiles across countries.

deterministic. Fig. 3 illustrates this by breaking down the composite index into its three components: hazard exposure, vulnerability, and lack of coping capacity, revealing distinct spatial patterns across cities.

This figure helps explain why several thermally stressed cities, including Kuala Lumpur (Malaysia), Bangkok (Thailand), Samut Prakan (Thailand), and Jeddah (Saudi Arabia), rank above the 90th percentile in hazard exposure yet do not fall within the top decile of composite risk (Fig. 3a–c). Their comparatively high coping capacity, including greater urban greening, and relatively lower energy costs (Fig. 3c), offset exposure and reduce their overall risk profile.

The findings show that even under conditions of high ambient heat, stronger coping capacity is associated with lower composite risk. However, it should be noted that these city-level scores derived from high-resolution data inevitably mask intra-urban inequalities: low-income households, informal settlement residents, and other marginalised groups with limited or no access to cooling, including air-conditioning, secure housing or wages, reliable energy, or green space may still face disproportionately high heat-related risks, even in cities that appear relatively well buffered on average.

3.3. *Vulnerability and coping deficits are key amplifiers of risk*

The heat-risk components of the top 10 highest-risk cities are presented in Fig. 4, with each city represented by a radar chart. The colours represent the dominant heat risk components across all panels: hazard exposure (orange), vulnerability (purple), and lack of coping capacity (blue). The dominant component is identified as the one with the highest normalised value. Cities with two or more similarly high component scores can be interpreted as having mixed risk profiles. This allows comparison of the dominant drivers of composite heat risk across cities. The complete list of cities is in Supplementary Note 1.

The results reveal that top-risk cities exhibit diverse pathways to elevated heat risk. Some cities like Al Basrah (Iraq) experience compounded risk across hazard exposure, vulnerability, and limited coping capacity, whereas in cities such as Bamako (Mali) and Kano (Nigeria), heat risk is driven primarily by demographic fragility, and in Faisalabad (Pakistan) and Hyderabad (Pakistan) by infrastructural and adaptive capacity deficits.

Notably, several cities with only moderate heat exposure below the 90th percentile are still ranked among the highest-risk urban areas due to compounding social and infrastructural vulnerabilities. Karachi (Pakistan), Faisalabad (Pakistan), and Kaduna (Nigeria) exemplify this pattern, with high scores in both vulnerability and lack of coping capacity. Contributing factors include high dependency ratios, low economic capacity, sparse urban vegetation, and limited access to cooling infrastructure.

For instance, Hyderabad (Pakistan) exhibits high risk despite relatively moderate hazard levels, driven by low economic capacity, sparse green cover, and elevated electricity costs. Similarly, Kano (Nigeria) ranks high in demographic vulnerability due to its large share of children under 4 years of age and low economic capacity to access adaptive technologies. These cases show how non-climatic factors can amplify risk, transforming moderate heat exposure into high composite risk.

3.4. *Sensitivity of results to methodological assumptions*

Sensitivity analyses indicate that the main findings are robust to alternative methodological choices. Under alternative weighting schemes, city rankings remain highly consistent with the baseline specification, and overlap in the top decile of highest-risk cities indicates

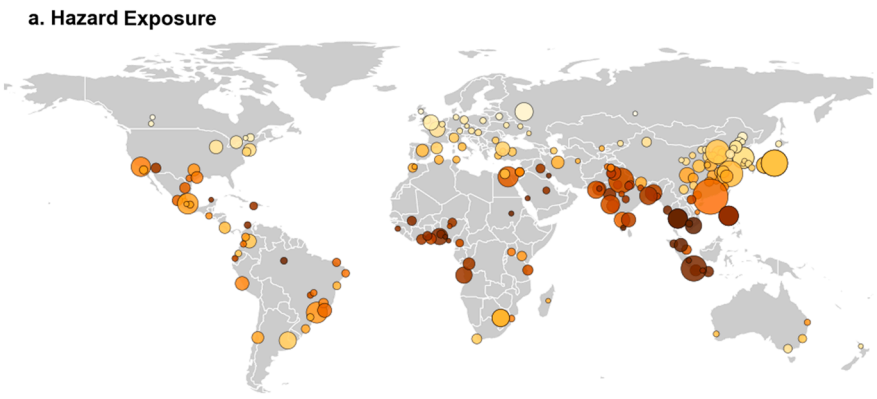

City	Country	Score
Ho Chi Minh City	Vietnam	1.0
Madurai	India	0.99
Bangkok	Thailand	0.98
Samut Prakan	Thailand	0.98
Phnom Penh	Cambodia	0.98
Kuala Lumpur	Malaysia	0.97
Khartoum	Sudan	0.96
Al Basrah	Iraq	0.96
Manaus	Brazil	0.96
Medan	Indonesia	0.96

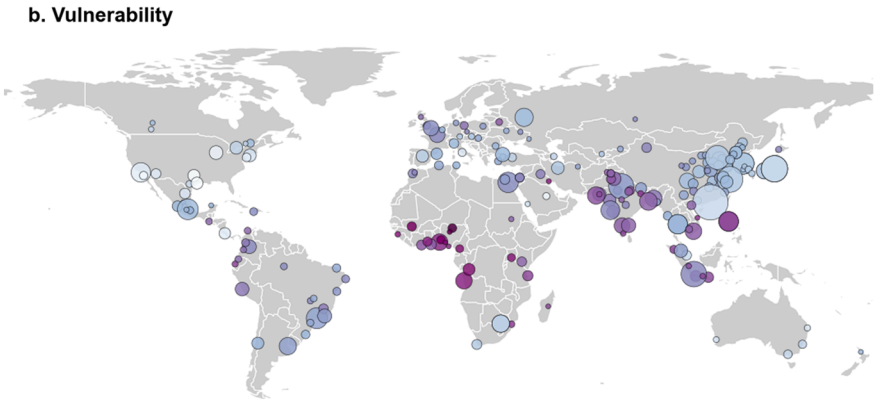

City	Country	Score
Kano	Nigeria	1.0
Kaduna	Nigeria	0.95
Bamako	Mali	0.9
Ibadan	Nigeria	0.88
Kinshasa	Congo, DRC	0.84
Benin City	Nigeria	0.84
Yaounde	Cameroon	0.84
Al Basrah	Iraq	0.83
Kampala	Uganda	0.83
Conakry	Guinea	0.83

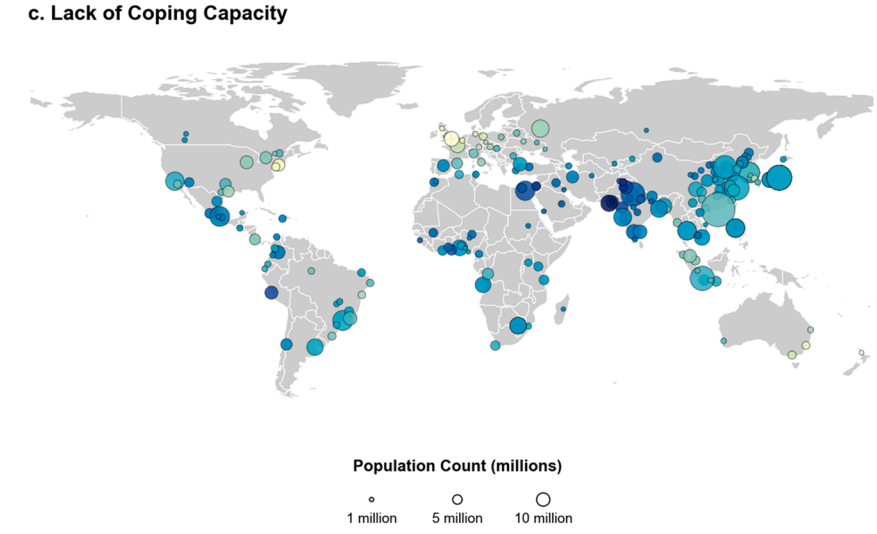

City	Country	Score
Karachi	Pakistan	1.0
Hyderabad	Pakistan	0.97
Faisalabad	Pakistan	0.89
Peshawar	Pakistan	0.88
Islamabad	Pakistan	0.87
Rawalpindi	Pakistan	0.87
Az Zarqa'	Jordan	0.83
Amman	Jordan	0.83
Lima	Peru	0.8
Lahore	Pakistan	0.8

Fig. 3. Global mapping of heat risk components across cities worldwide with populations exceeding 1 million in 2020: (a) hazard exposure, (b) vulnerability, and (c) lack of coping capacity. a, Hazard exposure represented by population-weighted cooling degree days derived from UTCI, together with land surface temperature anomalies that capture spatial thermal intensity. b, Vulnerability based on age structure, economic capacity, and fraction of air conditioning penetration. c, Lack of coping capacity captured through vegetation cover, and electricity costs. The bubble size represents the population. Each corresponding table highlights the top ten cities by component score. Values are normalised to a 0–1 scale.

that coping capacity plays a greater role in shaping risk outcomes when it is weighted more heavily than other factors, although substantial overlap persisted. Similarly, recalculating CDD_{UTCI} using 20°C and 22°C thresholds, instead of the baseline 18°C, altered the absolute magnitude of exposure but did not materially change the overall spatial patterns or the relative ordering of cities, indicating that the threshold serves primarily as a comparative index rather than a determinant of the main conclusions. Detailed results are reported in Supplementary Notes 3 and 4.

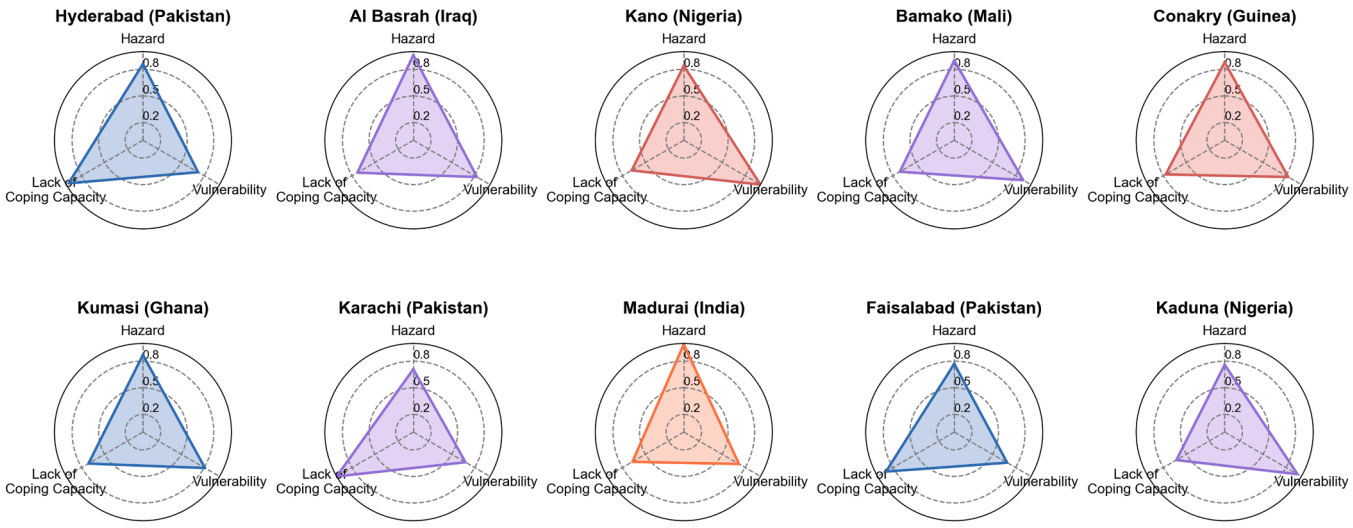

Fig. 4. Risk component profiles for the top 10 heat-risk cities. The colours represent the dominant heat risk components across all panels: hazard exposure (orange), vulnerability (purple), and lack of coping capacity (blue).

4. Discussion

Heat risk in cities is not solely determined by temperature extremes but by the combined effects of environmental conditions, including humidity, mean radiant temperature, wind speed, socio-demographic vulnerability and system-level capacity to cope. As a comparative diagnostic tool, the results suggest that global heat risk planning can benefit from moving beyond hazard-centric approaches toward component-targeted strategies that explicitly address hazard exposure, vulnerability, and coping capacity. In this context, the use of UTCI strengthens the analysis by providing a more physiologically meaningful representation of heat exposure and helps explain differences in risk across cities that are not evident from temperature-based metrics alone. The 18°C base threshold, commonly used in studies, should be interpreted as a standardised comparative benchmark rather than a location-specific heat–health threshold, particularly as sensitivity analysis using alternative weightings and thresholds indicates that this choice influences absolute magnitudes more than the relative ranking of risk across cities (Supplementary Notes 3 and 4).

More than 95% of cities above the 90th percentile risk are concentrated in South and Southeast Asia and Sub-Saharan Africa, where the urban populations are rapidly expanding, and resilient systems remain weak (Mora, Dousset, et al., 2017; Tuholske et al., 2021). This finding adds to recent projections indicating that the Global South will bear the brunt of future heat-related impacts due to overlapping exposure, vulnerability and limited coping capacity burdens (Grant et al., 2025; World Bank, 2025). These broad patterns are supported by evidence of increasing cooling demand and extreme heat exposure in the Global South (Lizana et al., 2026).

This global assessment goes beyond identifying hotspots of population exposure by explaining why risk diverges between cities with similar thermal profiles. Compared with prior exposure-dominant global assessments, this study advances the literature by combining globally harmonised hazard, vulnerability, and coping-capacity indicators within a single component-resolved framework, thereby enabling cross-city comparison not only of where heat risk is highest, but also of the distinct processes through which that risk is produced (ND-GAIN, 2021; Urban Climate Change Research Network (UCCRN), 2018).

Our globally harmonised, component-resolved approach reveals that some highly exposed cities to extreme heat, including Kuala Lumpur (Malaysia), Bangkok (Thailand), and Jeddah (Saudi Arabia), are buffered by relatively strong coping capacity, including higher vegetation cover (Y. Li et al., 2024; Yang et al., 2024), and more affordable energy (World Bank Group, 2021) for those who can afford it, preventing them from appearing in the highest risk decile. However, this apparent buffering should be interpreted with caution in relation to heat-related outcomes. For example, large-scale analyses show that heat-related mortality varies substantially across cities, even under comparable exposure conditions (Masselot et al., 2023), and is shaped by interacting stressors such as air pollution (Stafoggia et al., 2023) and the underlying population health (M. Chen et al., 2023). Lower composite risk in this analysis, therefore, reflects relative buffering capacity at the city scale rather than the absence of heat-related impacts. This highlights the importance of interpreting the present framework as a comparative diagnostic tool for understanding relative risk drivers, rather than as a direct predictor.

Conversely, several cities, including Karachi (Pakistan), Faisalabad (Pakistan), and Kaduna (Nigeria), face severe risk under moderate exposure due to the socio-economic vulnerability and infrastructural deficits. While air conditioning can reduce acute heat stress for those with access, reliance on it as a primary adaptation pathway is not sustainable, particularly given its high cost and energy-intensive requirements. Increased fossil fuel-based electricity demand, high global warming refrigerant gases, and waste heat emissions can exacerbate urban warming over time (Campbell et al., 2021; IPCC, 2023; Zhang et al., 2026). This highlights the importance of the sustainable cooling hierarchy, which puts forward passive cooling approaches and nature-based strategies, such as urban greening and shading, particularly in rapidly growing and resource-constrained cities, as the primary adaptation measures (Buo et al., 2023; Lizana et al., 2022; United Nations Environment Programme, 2025). In cities with higher coping capacity, greater access to cooling technologies and affordable electricity may increase reliance on energy-intensive adaptation measures such as air conditioning. While air conditioning can be essential during extreme heat, it may become maladaptive where passive and low-energy alternatives are sufficient (Khosla, 2025). Increased dependence on carbon-intensive cooling systems can raise energy demand, greenhouse gas emissions, and waste heat, potentially reinforcing long-term urban warming and heat risk (Calvin et al., 2023). Identifying local determinants of risk can therefore help inform adaptation strategies that reflect local priorities while accounting for long-term sustainability trade-offs.

In planning practice, component-specific risk profiles can help align interventions with dominant local risk drivers. Exposure-driven cities may prioritise urban climate-sensitive design measures that reduce thermal load, including shading, cool surfaces and ventilation corridors

(Buo et al., 2023; Y. Li et al., 2024). Vulnerability-driven cities may require stronger public-health and social-protection measures, including heat-health early warning systems and targeted support for heat-sensitive populations (Ebi et al., 2021; Kotharkar & Ghosh, 2022). When coping capacity is limited, priorities may include access to affordable cooling, electricity resilience, passive cooling, and urban greening (United Nations Environment Programme, 2025). This highlights the need for context-specific rather than uniform adaptation prescriptions.

Current urban heat adaptation measures range from public health outreach to early warning systems and targeted support for sensitive groups such as children, the elderly, and outdoor workers. In cities where institutional adaptation is lagging, the results suggest that strengthening coping capacity may represent an important area for further policy attention (Kotharkar & Ghosh, 2022; Y. Li et al., 2024; Yang et al., 2024). Analyses such as this study can help to inform and prioritise existing and new municipal heat action plans by indicating the relative roles and priorities among reducing exposure, reducing vulnerability, or increasing coping capacity. In practice, many cities, such as Ahmedabad (India) and Karachi (Pakistan), are already implementing coordinated heat plan measures such as advanced heat warnings, public communication, hydration points and surge capacity in health services. Ahmedabad's plan combines an early warning system, public awareness campaigns, health-system preparedness and targeted interventions such as cool roofs in low-income neighbourhoods, and has been associated with substantial reductions in heat-related mortality (Ahmedabad Municipal Corporation, 2019; Knowlton et al., 2014). Karachi's Heatwave Management Plan similarly sets out pre-, during- and post-event protocols, multi-agency coordination and communication strategies to protect vulnerable populations (Commissioner Karachi, 2017). Hyderabad in Sindh province (Pakistan), which ranks among our highest-risk cities, has recently been included in a provincial initiative to develop municipal heat action plans and establish temporary cooling and hydration points during extreme heat (Community Support Concern (CSSP), n.d.). By contrast, in other very high-risk cities in our study; Bamako (Mali), Al Basrah (Iraq), Kano (Nigeria) and Conakry (Guinea), available evidence highlights repeated severe heat impacts and high vulnerability, while documented city-level heat-action planning remains relatively limited, suggesting potential disparities between risk and implemented adaptation (Arrighi et al., 2025; Federal Ministry of Health (Nigeria), 2024; Global Center on Adaptation (GCA), 2022; World Bank, n.d.).

Future changes in climate, demographics, and socio-economic conditions are likely to reshape patterns of urban heat risk. Increasing heat extremes will intensify hazard exposure, while continued urban population growth and demographic ageing may increase vulnerability. At the same time, socio-economic development may enhance coping capacity through improved infrastructure and access to cooling, but uneven access could reinforce existing inequalities. Urban expansion and land-use change will further influence local heat conditions. Together, these trends suggest that future risk will depend not only on the changing climate but also on how vulnerability and coping capacity evolve. The present analysis, therefore, provides a cross-sectional baseline, with future work needed to extend this framework to dynamic, scenario-based assessments.

Finally, our results help identify where short-term investments in coping capacity may provide important entry points for strengthening longer-term adaptive capacity, indicating potential areas for policy attention. Integrated adaptation–mitigation strategies may support larger exposure reductions than either alone, consistent with the importance of strengthening coping capacity over time (Georgescu et al., 2023; Tuholske & Chapman, 2024).

4.1. Limitations of the study

Our analysis is based on harmonised 2019–2020 global datasets and population-weighted urban extents from LandScan (Patterson & Kelso, 2012). Although these urban extents may differ from administrative boundaries, they were selected for comparability across cities; future work could test alternative delineations (e.g., GHSL Urban Centres) (Florczyk et al., 2019). The framework emphasises coping capacity as a proxy for near-term resilience, while longer-term adaptive capacity (governance, institutional readiness) remains underrepresented due to data limitations. Importantly, the coping capacity indicators included in this study should not be interpreted as evidence of sustainable or low-carbon adaptation pathways, but rather as measures of short-term buffering capacity. In addition, several indicators also rely on broad proxies and may not capture local complexity; for example, electricity prices are based on national averages and should be interpreted as a comparative measure of cooling affordability rather than a city-specific indicator.

Although the sensitivity analyses indicate that the main results are robust to alternative weighting schemes, aggregation choices, and CDD thresholds, uncertainty remains due to methodological choices, including normalisation and weighting. No direct validation against independent outcome data was performed in the present study owing to the limited availability of globally comparable city-scale datasets on heat-related outcomes, including health (mortality and morbidity), economic impacts (heat-related losses), and environmental effects (energy demand and carbon emissions). The framework should therefore be interpreted as a comparative diagnostic tool for identifying relative risk drivers, rather than as a predictive model.

The study focuses on cities with populations exceeding one million, and the findings may not be directly generalisable to smaller urban areas or peri-urban contexts. While this global framework allows for cross-city comparison, it does not capture intra-urban heterogeneity, such as neighbourhood-scale variations in exposure, infrastructure, or social vulnerability, which are necessary for targeted hyper-local level heat adaptation responses. However, as climate extremes intensify and urbanisation accelerates, the framework offers a scalable basis for diagnosing heat risk in cities and supporting more context-sensitive adaptation planning.

5. Conclusion

This study presents a globally consistent, component-resolved assessment of heat risk in cities that moves beyond exposure-only approaches by integrating hazard, vulnerability, and coping capacity. Applied to 205 large cities (>1 million population), the framework enables direct comparison of both where risk is highest and the processes through which it arises. Based on the results, the following conclusions can be drawn:

First, the highest composite heat risks are strongly concentrated in South and Southeast Asia and Sub-Saharan Africa, with more than 95% of cities in the top decile of the risk distribution located in these regions, particularly in India, Pakistan, Nigeria and Ghana.

Second, hazard exposure alone is not predictive of overall risk, as some highly exposed cities like Bangkok (Thailand) and Jeddah (Saudi Arabia) rank lower due to strong coping capacity, rank lower in the composite index due to stronger coping capacity.

Third, vulnerability and coping deficits substantially amplify risk, such that cities with only moderate exposure can still rank among the highest risk where socio-economic and infrastructural constraints coincide, as observed in Karachi (Pakistan), Faisalabad (Pakistan) and Kaduna (Nigeria).

Finally, by disaggregating risk into its component drivers, the framework reveals distinct pathways through which heat risk emerges in cities within the same country, highlighting the need for targeted, context-specific adaptation strategies. These findings provide a basis for aligning interventions with local risk profiles and prioritising actions across exposure reduction, vulnerability alleviation, and capacity building.

Overall, this approach offers a scalable foundation for comparative heat risk assessment in cities. Future work should link such global analyses with finer-resolution local data and validation metrics, including heat-related outcomes, to better capture realised impacts and support more effective adaptation planning.

CRediT authorship contribution statement

Nethmi Jayaratne Kariyawasam: Writing – original draft, Visualization, Software, Resources, Methodology, Formal analysis, Data curation, Conceptualization. **Jesus Lizana:** Supervision. **Radhika Khosla:** Supervision.

Declaration of competing interest

The authors declare that they have no known competing financial interests or personal relationships that could have appeared to influence the work reported in this paper.

Acknowledgements

This research received support from the University of Oxford Strategic Research Fund and the Engineering and Physical Sciences Research Council (EPSRC). To ensure open access, we have granted a CC BY licence to any Author Accepted Manuscript resulting from this work.

Supplementary materials

Supplementary material associated with this article can be found, in the online version, at doi:10.1016/j.scs.2026.107535.

Appendix A. Composite risk results for the top 50 cities

City Name	Country Name	Total Population	Normalised Hazard Score	Normalised Vulnerability Score	Normalised LCA Score	Composite Risk score
Al Basrah	Iraq	1114933	0.96	0.83	0.73	0.83
Ahmadabad	India	6721469	0.89	0.57	0.79	0.79
Bamako	Mali	3807302	0.9	0.9	0.71	0.78
Nagpur	India	2350840	0.86	0.54	0.71	0.76
Quezon City	Philippines	17060195	0.87	0.73	0.55	0.70
Baghdad	Iraq	3638813	0.84	0.56	0.7	0.70
Madurai	India	1316792	0.99	0.72	0.67	0.73
Faisalabad	Pakistan	3770671	0.77	0.69	0.89	0.78
Lagos	Nigeria	12025166	0.91	0.8	0.57	0.76
Hyderabad	Pakistan	1366633	0.86	0.72	0.97	0.79
Barranquilla	Colombia	2043439	0.91	0.63	0.64	0.78
Ibadan	Nigeria	3003695	0.91	0.88	0.53	0.73
Port Harcourt	Nigeria	1004315	0.9	0.79	0.53	0.74
Conakry	Guinea	1369142	0.88	0.83	0.77	0.77
Bhopal	India	1457813	0.75	0.66	0.65	0.75
Ho Chi Minh City	Vietnam	12102505	1.00	0.66	0.57	0.70
Kaduna	Nigeria	1101425	0.76	0.95	0.63	0.74
Bandung	Indonesia	5640818	0.77	0.73	0.5	0.71
Port-au-Prince	Haiti	2756073	0.86	0.51	0.62	0.65
Kanpur	India	2949817	0.77	0.67	0.69	0.67
Luanda	Angola	12045280	0.85	0.81	0.58	0.72
Cairo	Egypt	18359205	0.68	0.51	0.76	0.69
Pune	India	6560440	0.74	0.62	0.66	0.66
Kinshasa	Congo, DRC	6394123	0.84	0.84	0.45	0.67
Manila	Philippines	17060195	0.87	0.73	0.55	0.69
Patna	India	1658600	0.75	0.77	0.72	0.73
Manaus	Brazil	2118792	0.96	0.52	0.39	0.66
Lahore	Pakistan	8440497	0.74	0.63	0.8	0.65
Abidjan	Cote d'Ivoire	4436144	0.84	0.68	0.58	0.71
Rawalpindi	Pakistan	2498182	0.59	0.64	0.87	0.69
Hyderabad	India	7781013	0.76	0.56	0.71	0.68
Accra	Ghana	5139757	0.77	0.65	0.76	0.7
Bangalore	India	10906703	0.64	0.65	0.68	0.69
Hanoi	Vietnam	3410323	0.75	0.63	0.58	0.65
Kolkata	India	14035780	0.82	0.64	0.59	0.66
Jaipur	India	3242035	0.78	0.62	0.77	0.7
Palembang	Indonesia	1321557	0.93	0.71	0.4	0.68
Bangkok	Thailand	16696153	0.98	0.38	0.52	0.61
Benin City	Nigeria	1003445	0.93	0.84	0.5	0.65
Dar es Salaam	Tanzania	4692228	0.74	0.73	0.54	0.7
Lucknow	India	3307272	0.73	0.68	0.7	0.68
Phnom Penh	Cambodia	2201647	0.98	0.66	0.69	0.73
Surabaja	Indonesia	4914370	0.94	0.71	0.49	0.72
Guayaquil	Ecuador	1644302	0.79	0.73	0.47	0.67
Mumbai	India	15544429	0.73	0.53	0.6	0.63
Goiania	Brazil	1771384	0.74	0.53	0.54	0.61
Merida	Mexico	1071416	0.89	0.39	0.54	0.58
Maputo	Mozambique	2034919	0.58	0.76	0.51	0.59
Chennai	India	9242295	0.79	0.64	0.62	0.64

Data availability

All analytical outputs generated in this study are provided in the Supplementary Information.

References

Ahmedabad Municipal Corporation. (2019). Ahmedabad heat action plan: Guide to extreme heat planning in Ahmedabad, India.

Arrighi, J., Izquierdo, K., Korodimou, M., Monasso, F., Pereira Marghidan, C., Singh, R., Amuron, I., Bahadur, A., Bailey, M., Jamie, C., Kadihasanoglu, A., Khan, R., Kiswendsida, G., Boyer, C., Ianni, F., Keith, L., Mistry, M., Khan, H., Design, E. R., … Wynter, A. (2025). Heat: through the eyes of the most vulnerable – Perceptions and pathways to action.

Bao, J., Li, X., & Yu, C. (2015). The construction and validation of the heat vulnerability index, a review. In *International Journal of Environmental Research and Public Health, 12* pp. 7220–7234). MDPI. https://doi.org/10.3390/ijerph120707220. Number 7.

Buo, I., Sagris, V., Jaagus, J., & Middel, A. (2023). High-resolution thermal exposure and shade maps for cool corridor planning. *Sustainable Cities and Society, 93*. https://doi.org/10.1016/j.scs.2023.104499

Calvin, K., Dasgupta, D., Krinner, G., Mukherji, A., Thorne, P. W., Trisos, C., Romero, J., Aldunce, P., Barrett, K., Blanco, G., Cheung, W. W. L., Connors, S., Denton, F., Diongue-Niang, A., Dodman, D., Garschagen, M., Geden, O., Hayward, B., Jones, C., & , … Ha, M., … (2023). *IPCC, 2023: Climate Change 2023: Synthesis Report. Contribution of Working Groups I, II and III to the Sixth Assessment Report of the Intergovernmental Panel on Climate Change [Core Writing Team, H. Lee and J. Romero (eds.)]*. Geneva, Switzerland: IPCC. https://doi.org/10.59327/IPCC/AR6-9789291691647

Campbell, Iain., Sachar, Sneha., Meisel, Julia., & Nanavatty, Rushad. (2021). *Beating the heat : a sustainable cooling handbook for cities*. United Nations Environment Programme.

Chakraborty, T., Hsu, A., Manya, D., & Sheriff, G. (2019). Disproportionately higher exposure to urban heat in lower-income neighborhoods: A multi-city perspective. In *Environmental Research Letters, 14*. Institute of Physics Publishing. https://doi.org/10.1088/1748-9326/ab3b99. Number 10.

Chen, M., Chen, L., Zhou, Y., Hu, M., Jiang, Y., Huang, D., Gong, Y., & Xian, Y. (2023). Rising vulnerability of compound risk inequality to ageing and extreme heatwave exposure in global cities. *Npj Urban Sustainability, 3*(1). https://doi.org/10.1038/s42949-023-00118-9

Chen, Z., O'Sullivan, K. C., Dohig, R. K., Pierse, N., Jiang, T., Riva, M., & Das, R. (2025). Identifying summer energy poverty and public health risks in a temperate climate. *Climate Risk Management, 48*. https://doi.org/10.1016/j.crm.2025.100698

CIBSE. (2006). Degree-Days: Theory and Application (TM41). Chartered Institution of Building Services Engineers.

Clarke, B., Konstantinoudis, G., Pinto, I., Barnes, C., Keeping, T., Otto, F., Gasparrini, A., Masselot, P., Mistry, M., Vicedo-Cabrera, A., & Theokritoff, E. (2025). Climate change tripled heat-related deaths in early summer European heatwave.

Commissioner Karachi. (2017). Karachi Heatwave Management Plan: A Guide to Planning and Response.

Community Support Concern (CSSP). (n.d.). Localized humanitarian actions & climate change: Heatwave response in Hyderabad. Retrieved November 19, 2025, from https://cssp.org.pk/localized-humanitarian-actions-climate-change/.

Creutzig, F., McPhearson, T., Bardhan, R., Belmin, C., Chow, W. T. L., Garschagen, M., Hsu, A., Kılkış, Ş., Islam, S. T., Milojevic-Dupont, N., Pathak, M., Pereira, R. H. M., Salehi, P., & Ürge-Vorsatz, D. (2025). Bridging the scale between the local particular and the global universal in climate change assessments of cities. *Nature Cities, 2*(5), 369–378. https://doi.org/10.1038/s44284-025-00226-w

Davis, L. W., & Gertler, P. J. (2015). Contribution of air conditioning adoption to future energy use under global warming. *Proceedings of the National Academy of Sciences of the United States of America, 112*(19), 5962–5967. https://doi.org/10.1073/pnas.1423558112

Davis, L., Gertler, P., Jarvis, S., & Wolfram, C. (2021). Air conditioning and global inequality. *Global Environmental Change, 69*. https://doi.org/10.1016/j.gloenvcha.2021.102299

Di Napoli, C., Pappenberger, F., & Cloke, H. L. (2018). Assessing heat-related health risk in Europe via the Universal Thermal Climate Index (UTCI). *International Journal of Biometeorology, 62*(7), 1155–1165. https://doi.org/10.1007/s00484-018-1518-2

Didan, K. (2015). *MOD13A3 MODIS/Terra vegetation Indices Monthly L3 Global 1km SIN Grid V006 [Data set]*. NASA Land Processes Distributed Active Archive Center. https://doi.org/10.5067/MODIS/MOD13Q1.006

Du, H., Zhan, W., Zhou, B., Ju, Y., Liu, Z., Middel, A., Huang, K., Zhao, L., Chakraborty, T., Wang, Z., Wang, S., Li, J., Li, L., Huang, F., Ji, Y., Li, X., & Li, M. (2025). Exacerbated heat stress induced by urban browning in the Global South. *Nature Cities, 2*(2), 157–169. https://doi.org/10.1038/s44284-024-00184-9

Ebi, K. L., Capon, A., Berry, P., Broderick, C., de Dear, R., Havenith, G., Honda, Y., Kovats, R. S., Ma, W., Malik, A., Morris, N. B., Nybo, L., Seneviratne, S. I., Vanos, J., & Jay, O. (2021). Hot weather and heat extremes: health risks. *The Lancet, 398* (10301), 698–708. https://doi.org/10.1016/S0140-6736(21)01208-3

Falchetta, G., Cian, E. De, Pavanello, F., & Wing, I. S (2024). Inequalities in global residential cooling energy use to 2050. *Nature Communications, 15*(1). https://doi.org/10.1038/s41467-024-52028-8

Federal Ministry of Health (Nigeria). (2024). Nigeria Climate Change and Health: National Vulnerability and Adaptation Assessment Report.

Florczyk A.J., Corbane C., Ehrlich D., Freire S., Kemper T., Maffenini L., Melchiorri M., Pesaresi M., Politis P., Schiavina M., Sabo F., & Zanchetta L. (2019). GHSL Data Package. https://doi.org/10.2760/290498.

Gasparrini, A., Guo, Y., Hashizume, M., Lavigne, E., Zanobetti, A., Schwartz, J., Tobias, A., Tong, S., Rocklöv, J., Forsberg, B., Leone, M., De Sario, M., Bell, M. L., Guo, Y. L. L., Wu, C. F., Kan, H., Yi, S. M., De Sousa Zanotti Stagliorio Coelho, M., Saldiva, P. H. N., … Armstrong, B. (2015). Mortality risk attributable to high and low ambient temperature: A multicountry observational study. *The Lancet, 386*(9991), 369–375. https://doi.org/10.1016/S0140-6736(14)62114-0

Georgescu, M., Broadbent, A. M., & Krayenhoff, E. S. (2023). Quantifying the decrease in heat exposure through adaptation and mitigation in twenty-first-century US cities. *Nature Cities, 1*(1), 42–50. https://doi.org/10.1038/s44284-023-00001-9

Global Center on Adaptation (GCA). (2022). State and Trends in Adaptation 2022: City Resilience – Conakry case study.

Grant, L., Vanderkelen, I., Gudmundsson, L., Fischer, E., Seneviratne, S. I., & Thiery, W. (2025). Global emergence of unprecedented lifetime exposure to climate extremes. *Nature, 641*(8062), 374–379. https://doi.org/10.1038/s41586-025-08907-1

Hondula, D. M., Balling, R. C., Vanos, J. K., & Georgescu, M. (2015). Rising Temperatures, Human Health, and the Role of Adaptation. *Current Climate Change Reports, 1*, 144–154. https://doi.org/10.1007/s40641-015-0016-4. Number 3.

International Panel on Climate Change (IPCC). (2023). *Climate Change 2022 – Impacts, Adaptation and Vulnerability: Working Group II Contribution to the Sixth Assessment Report of the Intergovernmental Panel on Climate Change*. Cambridge University Press.

IPCC. (2023). Summary for Policymakers. In: Climate Change 2023: Synthesis Report. Contribution of Working Groups I, II and III to the Sixth Assessment Report of the Intergovernmental Panel on Climate Change (P. Arias, M. Bustamante, I. Elgizouli, G. Flato, M. Howden, C. Méndez-Vallejo, J. J. Pereira, R. Pichs-Madruga, S. K. Rose, Y. Saheb, R. Sánchez Rodríguez, D. Ürge-Vorsatz, C. Xiao, N. Yassaa, J. Romero, J. Kim, E. F. Haites, Y. Jung, R. Stavins, … Y. Park, Eds.). https://doi.org/10.59327/IPCC/AR6-9789291691647.001.

Jian, H., Yan, Z., Fan, X., Zhan, Q., Xu, C., Bei, W., Xu, J., Huang, M., Du, X., Zhu, J., Tai, Z., Hao, J., & Hu, Y. (2024). A high temporal resolution global gridded dataset of human thermal stress metrics. *Scientific Data, 11*(1). https://doi.org/10.1038/s41597-024-03966-x

Jones, N. (2025). Urban Heat: Assessing Risks and Identifying Interventions. City Climate Finance Gap Fund Technical Note.

Khosla, R. (2025). *The Role of Cooling Standards in Climate Adaptation to Extreme Heat*. World Bank Working Paper.

Klein, T., & Anderegg, W. R. L. (2021). A vast increase in heat exposure in the 21st century is driven by global warming and urban population growth. *Sustainable Cities and Society, 73*. https://doi.org/10.1016/j.scs.2021.103098

Knowlton, K., Kulkarni, S. P., Azhar, G. S., Mavalankar, D., Jaiswal, A., Connolly, M., Nori-Sarma, A., Rajiva, A., Dutta, P., Deol, B., Sanchez, L., Khosla, R., Webster, P. J., Toma, V. E., Sheffield, P., & Hess, J. J. (2014). Development and implementation of South Asia's first heat-health action plan in Ahmedabad (Gujarat, India). *International Journal of Environmental Research and Public Health, 11*(4), 3473–3492. https://doi.org/10.3390/ijerph110403473

Kotharkar, R., & Ghosh, A. (2022). Progress in extreme heat management and warning systems: A systematic review of heat-health action plans (1995-2020). In *Sustainable Cities and Society, 76*. Elsevier Ltd. https://doi.org/10.1016/j.scs.2021.103487

Kumari, RM., & Kitchley, J. L (2024). A framework to assess the contextual composite heat vulnerability index for a heritage city in India- A case study of Madurai. *Sustainable Cities and Society,, 101*. https://doi.org/10.1016/j.scs.2023.105119

Kummu, M., Kosonen, M., & Masoumzadeh Sayyar, S. (2025). Downscaled gridded global dataset for gross domestic product (GDP) per capita PPP over 1990–2022. *Scientific Data, 12*(1), 178. https://doi.org/10.1038/s41597-025-04487-x

Li, D., & Bou-Zeid, E. (2013). Synergistic Interactions between Urban Heat Islands and Heat Waves: The Impact in Cities Is Larger than the Sum of Its Parts. *Journal of Applied Meteorology and Climatology, 52*(9), 2051–2064. https://doi.org/10.1175/JAMC-D-13-02.s1

Li, F., Yigitcanlar, T., Nepal, M., Nguyen, K., Dur, F., & Li, W. (2024). Assessing heat vulnerability and multidimensional inequity: Lessons from indexing the performance of Australian capital cities. *Sustainable Cities and Society, 115*. https://doi.org/10.1016/j.scs.2024.105875

Li, Y., Svenning, J. C., Zhou, W., Zhu, K., Abrams, J. F., Lenton, T. M., Ripple, W. J., Yu, Z., Teng, S. N., Dunn, R. R., & Xu, C. (2024). Green spaces provide substantial but unequal urban cooling globally. *Nature Communications, 15*(1). https://doi.org/10.1038/s41467-024-51355-0

Liu, Y., Liu, R., Chen, J., Wei, X., Qi, L., & Zhao, L. (2024). A global annual fractional tree cover dataset during 2000–2021 generated from realigned MODIS seasonal data. *Scientific Data, 11*(1). https://doi.org/10.1038/s41597-024-03671-9

Lizana, J., Miranda, N. D., Gross, L., Mazzone, A., Cohen, F., Palafox-Alcantar, G., Fahr, P., Jani, A., Renaldi, R., McCulloch, M., & Khosla, R. (2022). Overcoming the incumbency and barriers to sustainable cooling. *Buildings and Cities, 3*(1), 1075–1097. https://doi.org/10.5334/bc.255

Lizana, J., Miranda, N. D., Sparrow, S. N., Wallom, D. C. H., Khosla, R., & McCulloch, M. (2026). Global gridded dataset of heating and cooling degree days under climate change scenarios. *Nature Sustainability, 9*(3), 470–480. https://doi.org/10.1038/s41893-025-01754-y

Mah, J. C., Penwarden, J. L., Pott, H., Theou, O., & Andrew, M. K. (2023). Social vulnerability indices: a scoping review. *BMC Public Health, 23*(1). https://doi.org/10.1186/s12889-023-16097-6

Masselot, P., Mistry, M., Vanoli, J., Schneider, R., Iungman, T., Garcia-Leon, D., Ciscar, J. C., Feyen, L., Orru, H., Urban, A., Breitner, S., Huber, V., Schneider, A., Samoli, E., Stafoggia, M., de'Donato, F., Rao, S., Armstrong, B., Nieuwenhuijsen, M., … Aunan, K. (2023). Excess mortality attributed to heat and cold: a health impact

assessment study in 854 cities in Europe. *The Lancet Planetary Health, 7*(4), e271–e281. https://doi.org/10.1016/S2542-5196(23)00023-2

Mazzone, A., De Cian, E., Falchetta, G., Jani, A., Mistry, M., & Khosla, R. (2023). Understanding systemic cooling poverty. *Nature Sustainability*. https://doi.org/10.1038/s41893-023-01221-6

Mitchell, D., Heaviside, C., Vardoulakis, S., Huntingford, C., Masato, G. P, Guillod, B., Frumhoff, P., Bowery, A., Wallom, D., & Allen, M. (2016). Attributing human mortality during extreme heat waves to anthropogenic climate change. *Environmental Research Letters, 11*(7). https://doi.org/10.1088/1748-9326/11/7/074006

Mora, C., Counsell, C. W. W., Bielecki, C. R., & Louis, L. V. (2017). Twenty-seven ways a heat wave can kill you: Deadly heat in the era of climate change. *Circulation: Cardiovascular Quality and Outcomes, 10*(11). https://doi.org/10.1161/CIRCOUTCOMES.117.004233

Mora, C., Dousset, B., Caldwell, I. R., Powell, F. E., Geronimo, R. C., Bielecki, C. R., Counsell, C. W. W., Dietrich, B. S., Johnston, E. T., Louis, L. V., Lucas, M. P., Mckenzie, M. M., Shea, A. G., Tseng, H., Giambelluca, T. W., Leon, L. R., Hawkins, E., & Trauernicht, C. (2017). Global risk of deadly heat. *Nature Climate Change, 7*(7), 501–506. https://doi.org/10.1038/nclimate3322

ND-GAIN. (2021). *Urban Adaptation Assessment (UAA) Dataset*. University of Notre Dame. https://gain.nd.edu/our-work/global-urban-climate-assessment/.

Palermo, V., Hernandez Moral, G., Treville, A., Barbosa, P., & Melica, G.,. (2025). How to develop a risk and vulnerability assessment - Covenant of Mayors Guidebook Complementary document 2. https://doi.org/10.2760/5760528.

Patterson, Tom., & Kelso, N. V. (2012). World Urban Areas, LandScan, 1:10 million. World Urban Areas, LandScan, 1:10 Million (2012). https://purl.stanford.edu/yk247bg4748.

Rathi, S. K., Chakraborty, S., Mishra, S. K., Dutta, A., & Nanda, L. (2022). A heat vulnerability index: Spatial patterns of exposure, sensitivity and adaptive capacity for urbanites of four cities of India. *International Journal of Environmental Research and Public Health, 19*(1). https://doi.org/10.3390/ijerph19010283

Rocha, A. D., Vulova, S., Förster, M., Gioli, B., Matthews, B., Helfter, C., Meier, F., Steeneveld, G.-J., Barlow, J. F., Järvi, L., Chrysoulakis, N., Nicolini, G., & Kleinschmit, B. (2024). Unprivileged groups are less served by green cooling services in major European urban areas. *Nature Cities, 1*(6), 424–435. https://doi.org/10.1038/s44284-024-00077-x

Stafoggia, M., Michelozzi, P., Schneider, A., Armstrong, B., Scortichini, M., Rai, M., Achilleos, S., Alahmad, B., Analitis, A., Åström, C., Bell, M. L., Calleja, N., Krage Carlsen, H., Carrasco, G., Paul Cauchi, J., DSZS Coelho, M., Correa, P. M., Diaz, M. H., Entezari, A., … de' Donato, F. K. (2023). Joint effect of heat and air pollution on mortality in 620 cities of 36 countries. *Environment International, 181*. https://doi.org/10.1016/j.envint.2023.108258

Tuholske, C., Caylor, K., Funk, C., Verdin, A., Sweeney, S., Grace, K., Peterson, P., & Evans, T. (2021). Global urban population exposure to extreme heat. https://doi.org/10.1073/pnas.2024792118/-/DCSupplemental.

Tuholske, C., & Chapman, H. (2024). How to cool American cities. *Nature Cities, 1*(1), 16–17. https://doi.org/10.1038/s44284-023-00017-1

Uejio, C. K., Wilhelmi, O. V., Golden, J. S., Mills, D. M., Gulino, S. P., & Samenow, J. P. (2011). Intra-urban societal vulnerability to extreme heat: The role of heat exposure and the built environment, socioeconomics, and neighborhood stability. *Health and Place, 17*(2), 498–507. https://doi.org/10.1016/j.healthplace.2010.12.005

United Nations Department of Economic and Social Affairs. (2019). World Population Prospects 2019 Highlights.

United Nations Environment Programme. (2025). Global Cooling Watch 2025: The free degrees: How sustainable passive-first cooling can save lives, money and food. https://doi.org/10.59117/20.500.11822/48926.

Urban Climate Change Research Network (UCCRN). (2018). The Future We Don't Want: How Climate Change Could Impact the World's Greatest Cities. https://www.c40.org/wp-content/uploads/2023/04/1789_Future_We_Dont_Want_Report_1.4_hi-res_120618.original-compressed.pdf.

Vaňo, S., Duchková, H., Bašta, P., Jančovič, M., Geletič, J., Lorencová, E. K., & Suchá, L. (2025). From scenarios to strategies. Integrated methodology addressing urban heat vulnerability in uncertain future. *Sustainable Cities and Society, 106202*. https://doi.org/10.1016/j.scs.2025.106202

Varquez, A. C. G., Taerakul, J., Renard, F., Alonso, L., Choi, S., Hiroki, R., Ashie, Y., Kumakura, E., Okumura, M., Hanaoka, S., Inagaki, A., & Kanda, M. (2025). High-resolution outdoor heat-risk modeling for city central areas with applications to Tokyo and Lyon. *Sustainable Cities and Society, 125*. https://doi.org/10.1016/j.scs.2025.106344

Vernaccini, M., & Poljansek, L. (2017). INFORM Index for Risk Management. https://doi.org/10.2760/094023.

Voelkel, J., Hellman, D., Sakuma, R., & Shandas, V. (2018). Assessing vulnerability to urban heat: A study of disproportionate heat exposure and access to refuge by socio-demographic status in Portland, Oregon. *International Journal of Environmental Research and Public Health, 15*(4). https://doi.org/10.3390/ijerph15040640

Wan, Z., Hook, S., & Hulley, G. (2021). MODIS/Terra Land Surface Temperature/Emissivity Monthly L3 Global 0.05Deg CMG V061 [Data set]. *NASA Land Processes Distributed Active Archive Center*. https://doi.org/10.5067/MODIS/MOD11C3.061

Watts, N., Adger, W. N., Ayeb-Karlsson, S., Bai, Y., Byass, P., Campbell-Lendrum, D., Colbourn, T., Cox, P., Davies, M., Depledge, M., Depoux, A., Dominguez-Salas, P., Drummond, P., Ekins, P., Flahault, A., Grace, D., Graham, H., Haines, A., Hamilton, I., … Costello, A. (2017). The Lancet Countdown: tracking progress on health and climate change. In *The Lancet, 389* pp. 1151–1164). Lancet Publishing Group. https://doi.org/10.1016/S0140-6736(16)32124-9. Number 10074.

World Bank. (2025). Handbook on Urban Heat Management in the Global South. www.worldbank.org.

World Bank. (n.d.). Climate Change Knowledge Portal: Iraq – Heat Risk. Retrieved November 19, 2025, from https://climateknowledgeportal.worldbank.org/country/iraq/heat-risk.

World Bank Group. (2021). Doing Business project. https://databank.worldbank.org/id/7b12e700.

WorldPop. (2018). - School of Geography and Environmental Science, University of Southampton; Department of Geography and Geosciences, University of Louisville; Departement de Geographie, Universite de Namur), & Center for International Earth Science Information Network (CIESIN), C. U. www.worldpop.org. Global High Resolution Population Denominators Project - Funded by The Bill and Melinda Gates Foundation (OPP1134076). 10.5258/SOTON/WP00647.

Wu, X., Wang, J., Ge, Y., Lai, S., Zhang, D., Ren, Z., & Wang, J. (2025). Future heat-related mortality in Europe driven by compound day-night heatwaves and demographic shifts. *Nature Communications, 16*(1). https://doi.org/10.1038/s41467-025-62871-y

Xiang, Z., Qin, H., He, B. J., Han, G., & Chen, M. (2022). Heat vulnerability caused by physical and social conditions in a mountainous megacity of Chongqing, China. *Sustainable Cities and Society, 80*. https://doi.org/10.1016/j.scs.2022.103792

Xu, Y., Zhang, W., Wei, M., & Hong, T. (2025). Mapping heat vulnerability in cities: A tale of two california cities. *Sustainable Cities and Society, 135*. https://doi.org/10.1016/j.scs.2025.107002

Yang, M., Ren, C., Wang, H., Wang, J., Feng, Z., Kumar, P., Haghighat, F., & Cao, S.-J. (2024). Mitigating urban heat island through neighboring rural land cover. *Nature Cities, 1*(8), 522–532. https://doi.org/10.1038/s44284-024-00091-z

Ye, J., & Yang, F. (2025). Towards multi-scale and context-specific heat health risk assessment - A systematic review. In *Sustainable Cities and Society, 119*. Elsevier Ltd. https://doi.org/10.1016/j.scs.2024.106102

Zhang, H., Shan, Y., Li, R., Xue, R., Ma, J., Kikstra, J., Shi, Z., Wang, Z., Zhang, B., Wang, B., Fang, S., Yang, F., & Hubacek, K. (2026). Rising Air-Conditioning Use Intensifies Global Warming. *Nature Communications, 17*(1). https://doi.org/10.1038/s41467-026-69393-1

Zhao, L., Oppenheimer, M., Zhu, Q., Baldwin, J. W., Ebi, K. L., Bou-Zeid, E., Guan, K., & Liu, X. (2018). Interactions between urban heat islands and heat waves. *Environmental Research Letters, 13*(3). https://doi.org/10.1088/1748-9326/aa9f73

Zhao, N., Liu, Y., Cao, G., Samson, E. L., & Zhang, J. (2017). Forecasting China's GDP at the pixel level using nighttime lights time series and population images. *GIScience and Remote Sensing, 54*(3), 407–425. https://doi.org/10.1080/15481603.2016.1276705